Journal of Chromatography A, 1218 (2011) 2438–2444

Contents lists available at ScienceDirect

Journal of Chromatography A

journal homepage: www.elsevier.com/locate/chroma

Characterisation of methacrylate monoliths for bacteriophage purification

Franc Smrekar[a], Mateja Ciringer[a,b], Aleš Štrancar[a], Aleš Podgornik[a,b,*]

[a] BIA Separations d.o.o., Teslova 30, SI-1000 Ljubljana, Slovenia
[b] The Centre of Excellence for Biosensors, Instrumentation and Process Control – COBIK, Velika pot 22, SI-5250 Solkan, Slovenia

ARTICLE INFO

Article history:
Available online 25 December 2010

Keywords:
Bacteriophage
Purification
Monoliths
Layer thickness
Capacity
CIM

ABSTRACT

Binding of three different bacteriophages (phages), namely T7, lambda and M13 on methacrylate monoliths was investigated. Phage M13 exhibited the highest dynamic binding capacity of 4.5×10^{13} pfu/mL while T7 and lambda showed capacity of 1×10^{13} pfu/mL, all corresponding to values of around 1 mg/mL. Interestingly, capacity for lambda phage was increased 5-fold by increasing NaCl concentration in a loaded sample from 0 to 0.2 M while there was a constant capacity decrease for T7 and M13 phages. Under optimal conditions, recovery for all three phages approached 100%. Measurement of a pressure drop increase during loading enabled estimation of adsorbed phage layer thickness. At a maximal capacity it was calculated to be around 50 nm for T7 phage and 60 nm for lambda phage matching closely capside size thus indicating monolayer adsorption while 80 nm layer thickness was estimated for M13 phage showing its orientation along the pore.

1. Introduction

Bacteriophages (phages) are becoming increasingly studied subject due to several important properties. As natural enemies of bacteria they can serve as a substitute for antibiotics [1]. In addition, there are many other applications where they are used such as a detection tool for pathogenic organisms, delivery vehicle for proteins and DNA vaccines, gene therapy delivery vehicle, and a tool for screening libraries of proteins so-called phage display [2]. Especially phage display developed in 1985 by Smith [3] is an exponentially growing field in last 25 years [4] increasing demand for pure phages. In addition, phage production for phage therapy in Soviet union already in 1980s exceeded 2 tonnes [5] and recent progresses in many areas, including several clinical trials, will probably require even higher quantities of purified phages. Traditionally, purification of phages was based on centrifugation [6] but high purity and reproducibility of the phage formulation demanded for human treatment are the driving forces for the application of different purification protocols. An obvious option is chromatography, which enables preparation of the samples to a very high degree of purity. First report in using chromatography for phage purification dates back to 1957 [7] when Creaser and Taussig applied anion-exchange cellulose for purification of phages T1 and T2 from an *Escherichia coli* lysate. In 1973 Sundberg and Hoglund purified T4 phage on polylysine agarose [8] and in early 1980s anion exchange membrane chromatography [9,10] and gel chromatography were implemented [11]. For the last 25 years chromatography was one of the drivers of phage display libraries' development. However, amounts of phages to be purified were rather small therefore purification productivity was not the main issue. For large phage quantity production however, this became a very important factor and one of the key parameters, determining chromatographic purification process productivity is resin dynamic binding capacity (DBC). While many traditional particle based resins suffer from rather low DBC for very large molecules, monoliths exhibit high capacity for extremely large molecules like plasmid DNA and viruses [12]. Considering that the resolution and capacity are flow-unaffected, they seem to be a matrix of choice for phage purification especially in ion-exchange interaction (IEX) mode where mild elution conditions are applied. Suitability of monoliths for phage concentration and purification was already demonstrated by Smrekar et al. [13] and Kramberger et al. [14] implementing methacrylate CIM monoliths, while Noppe et al. [15,16] used cryogel monoliths for phage immobilization thus making an affinity column using phage as a ligand.

Using IEX chromatography mode DBC commonly decreases exponentially with an increase of ionic strength in the loading sample [17,18]. This can be a problem since most of the fermentation broths, from which a target product is to be purified, contains substantial amount of salts that can easily reach values up to 0.3 M NaCl [19,20]. However, for very large molecules it was theoretically predicted, that salt addition during loading can neutralize repulsion forces between charged macromolecules, which can consequently be adsorbed more densely on the chromatographic surface resulting in higher capacity [21]. While this was first demonstrated for

* Corresponding author at: BIA Separations d.o.o., Teslova 30, SI-1000 Ljubljana, Slovenia. Tel.: +386 1 426 56 49; fax: +386 1 426 56 50.
E-mail address: ales.podgornik@monoliths.com (A. Podgornik).

0021-9673/$ – see front matter © 2010 Elsevier B.V. All rights reserved.
doi:10.1016/j.chroma.2010.12.083

large proteins [21] it was also found to be true for DNA [22,23] and virus particles [24]. In all cases there was a very shallow optimum or even constant DBC value from a very low ionic strength till NaCl concentration of around 0.2–0.3 M, followed by a substantial DBC decrease at higher salt concentrations. Recently however, experiments with 40 kbp large plasmids demonstrated a 6-fold increase of DBC with the increase of salt concentration, having maximum at around 0.4 M NaCl [25]. Further investigation revealed similar trends for even larger plasmid of 60 kbp [26], while small plasmid of 5 kbp exhibited almost constant DBC up to 0.2 M [23].

In this work we investigated effect of loading conditions on methacrylate monolith DBC and recovery for three phages T7, lambda and M13. Measurement of pressure drop was used to estimate adsorption behavior.

2. Materials and methods

2.1. Materials

Bacteriophage T7 and its host bacteria *E. coli* (strain BL21) were purchased from Novagen (Merck, Darmstadt, Germany). Lambda phage with *E. coli* strain DSM 4230 was purchased from DSMZ (Braunschweig, Germany). Bacteriophage M13 was selected as previously described [27]. Phage library with complexity on the order of 10^9 independent clones and *E. coli* host strain ER2738 were purchased from New England Biolabs (Ipswich, MA, USA). Luria–Bertani medium (LB medium), Tris, sodium chloride, sodium hydroxide, and hydrochloric acid (37%) were obtained from Merck (Darmstadt, Germany). All solutions were prepared using water purified by a Watek IWA80 roi (Ledec and Sazavou, Czech Republic) water purification system and analytical grade reagents. Buffer solutions were prepared by dissolving a defined mass of buffer salt, pH was adjusted using HCl or NaOH. pH was measured using MA 5736 pH meter (Metrel, Horjul, Slovenia) with InLab 406 combination pH electrode (Mettler Toledo, Urdorf, Switzerland). Finally, buffers were filtered through a 0.45 μm pore size filter composed of Sartolon polyamide (Sartorius, Goettingen, Germany). All CIM monolithic columns, 0.34 mL disk column and 0.034 mL analytical column prototype packed into commercially available disk housing or specially designed POM housing for 0.034 mL columns, were obtained from BIA Separations (Ljubljana, Slovenia).

Cell density was measured by spectrophotometer Smart Spec 3000 (BioRad, Richmond, VI, USA), sample centrifugations were performed using Sorvall RC5C Plus centrifuge (Kendro, Newtown, CT, USA). All chromatographic experiments were performed using a gradient Knauer HPLC system (Berlin, Germany) consisting of two Knauer Type 64 analytical pumps, an injection valve with 100 μL sample loops, a Knauer UV–vis absorbance detector model K-2500 with a 10 mm optical path cell and a conductivity monitor Amersham Biosciences (GE Healthcare, Uppsala, Sweden), all connected via a Knauer interface box to a personal computer for real time data acquisition by Eurochrom 2000 software. During capacity measurements pressure drop on the monolithic columns was measured by differential manometer (MidWest Instruments, Sterling Heights, MI, USA).

2.2. Methods

2.2.1. Sample preparation

Phages were propagated using LB medium, which was primarily inoculated with phage specific *E. coli* strain. By OD 0.4 fermentation broth was inoculated with phages. After all bacteria were lysed in case of T7 and lambda phage or after 3 h in case of phage M13, suspension was centrifuged for 20 min at 6000 × *g* and 4 °C in a centrifuge (Sigma, Osterode am Harz, Germany). Afterwards, supernatant was filtered through 0.45 μm pore size filter (Millipore, Billerica, MA, USA) and kept at 4 °C. Purification and plaque assay procedures for determination of phage titer are described elsewhere [13].

2.2.2. Capacity and recovery determination

Dynamic binding capacity (DBC) was analyzed using custom made CIM QA monolithic columns of 34 μL monolith volume with various ligand densities but conventional structure (pore radius 730 nm). Different ionic strengths of the mobile phase containing phages used during loading were prepared by addition of appropriate volume of Tris–HCl buffer (pH 7.5) containing 2 M NaCl. The sample was loaded onto equilibrated monolithic column using HPLC pumps. Measurement of a phage titer of the loading solution was used to determine the phage concentration while a phage titer in the flow-through fractions enabled determination of the breakthrough curve. DBC was determined at 10% of the breakthrough curve. Phages were then eluted using stepwise gradient to the Tris–HCl buffer containing 1 M NaCl and fractions were collected. Phage titer of each collected fraction was multiplied with the fraction volume and values of all fractions were summarized to get the total amount of eluted viable phage. Recovery was calculated as a ratio between eluted and loaded phage amounts.

2.2.3. Pressure drop measurement and estimation of adsorbed layer thickness

Thickness of adsorbed layer was estimated from equation [23,26]:

$$h = r \cdot \left(1 - \sqrt{\frac{\sqrt{\varepsilon^2 \cdot (B_A/B) + 4 \cdot \sqrt{B_A/B} \cdot (1-\varepsilon)} - \varepsilon \cdot \sqrt{B_A/B}}{2 \cdot (1-\varepsilon)}} \right) \quad (1)$$

where h is adsorbed layer thickness (nm), r is the pore radius (nm), ε is the column porosity, B and B_A are clean and loaded monolith permeabilities (m^2) calculated from equation:

$$\frac{1}{B} = \frac{\Delta P}{\eta L u} \quad (2)$$

where ΔP is the pressure drop on the monolith (Pa), L is the monolith length (m), η is the mobile phase viscosity (Pa s) and u is the superficial velocity (m/s) calculated as $u = \phi_V/S$ (ϕ_V is the volume flow rate (m^3/s) and S is the cross sectional area of the monolith (m^2)).

2.2.4. Determination of the surface coverage

To calculate surface coverage by the phage at its maximal loaded amount on the monolith, the phage dimensions from literature were used: for filamentous phage M13 length of 930 nm and thickness of 6.5 nm [28], for lambda phage the capside diameter of 60 nm and the tail length of 120 nm [29,30] and for T7 phage the capside diameter of 50 nm and very small tail [31]. We assumed that a single phage particle covers the area of its maximal length (capside diameter + tail length for lambda phage) and its maximal thickness (capside diameter for lambda and T7). Multiplying surface covered by a single phage particle by the maximal obtained DBC, assuming that the monolith surface area is 7.19 m^2/g [32] and the monolith density 0.5 g/mL, the surface coverage was calculated to be 7.6%, 3.3% and 0.8% for phages M13, lambda and T7, respectively.

3. Results and discussion

Three different bacteriophages were selected, differing in their shape and size as described in details in Section 2.2.4. To establish binding-elution conditions and to verify if selected phages,

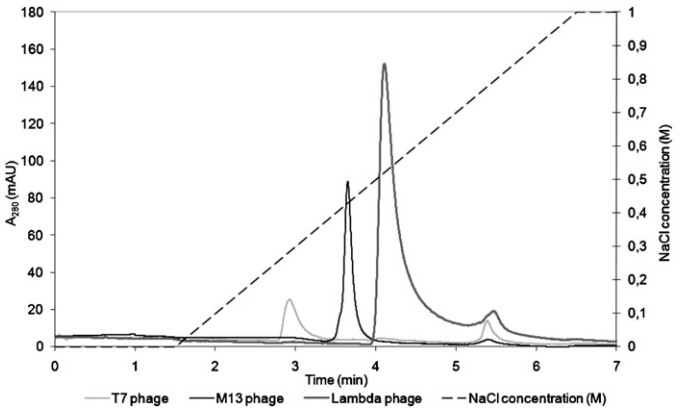

Fig. 1. Separation of T7, M13 and lambda phages using CIM QA monolithic column. Conditions: Stationary phase: 0.34 mL CIM QA disk monolithic column; mobile phase: buffer A: 20 mM Tris, pH 7.5; buffer B: 20 mM Tris, 1.0 M NaCl, pH 7.5; gradient: linear gradient from 0 to 100% buffer B in 5 min; flow rate: 4 mL/min; injection volume: 0.1 mL; detection: UV at 280 nm.

because of their size, cause any blocking of the monolithic column, we injected purified samples of all three phages onto the monolithic anion exchange QA column using Tris–HCl buffer, pH 7.5 as a mobile phase. Data is shown in Fig. 1. All three phages bind to the column and are eluted using NaCl gradient with 100% recovery while no blocking or pressure increase on the column was observed. Since they do elute at different NaCl concentrations it is even possible to separate selected phages when they are mixed together.

Because of high recovery achieved during injection of phages on QA monolithic column this matrix can be implemented for their purification. Therefore, we investigated how various factors influence phage capacity and recovery. Recently it was reported that addition of NaCl during loading significantly affects capacity of large plasmid DNA [25]. To investigate if this is the case also with phages we separately loaded on the column all three purified phages at different NaCl concentrations in the loading buffer. Data is summarized in Fig. 2.

Three phages do exhibit substantially different capacity profiles when loaded at different NaCl concentrations. Phage T7 DBC exhibited the highest capacity of approximately 1×10^{13} pfu/mL in the absence of NaCl. This corresponds to the mass capacity of 0.9 mg/mL taking in to account phage molecular weight of 5×10^7 Da [33]. By increasing NaCl concentration there was an exponential decrease of DBC typical for proteins [17,18]. At 0.1 M NaCl concentration having similar ionic strength as LB medium normally used as an *E. coli* growth medium, capacity decreased by twofold while loading at 0.18 M NaCl resulted in only one tenth of maximal DBC. Much higher initial capacity of 4.5×10^{13} pfu/mL DBC was measured for M13 phage. However, due to lower molecular weight of 1.6×10^7 Da [34] mass capacity was only slightly higher being 1.2 mg/mL. Profile of capacity values when changing NaCl concentration in the loading sample was similar to T7 phage but capacity decrease was substantially smaller, only for about 30% at 0.2 M NaCl. Despite the M13 hair-like shape, which resembles to a supercoiled form of plasmid DNA, profile of capacity values when changing NaCl concentration in the loading sample was completely different of those found for large plasmids [25]. On the other hand, lambda capacity profile when changing NaCl concentration in the loading sample was very different, exhibiting clear optimum at the salt concentration of 0.2 M with capacity similar to T7 phage of 1×10^{13} pfu/mL or 1 mg/mL when the molecular weight of 5.7×10^7 Da is assumed [35]. A 5-fold DBC increase was achieved when compared to loading without NaCl. This data is very similar in trend to the data obtained for 40 kbp plasmid [25], the main difference is that in the case of phage, optimum was achieved at lower salt concentration.

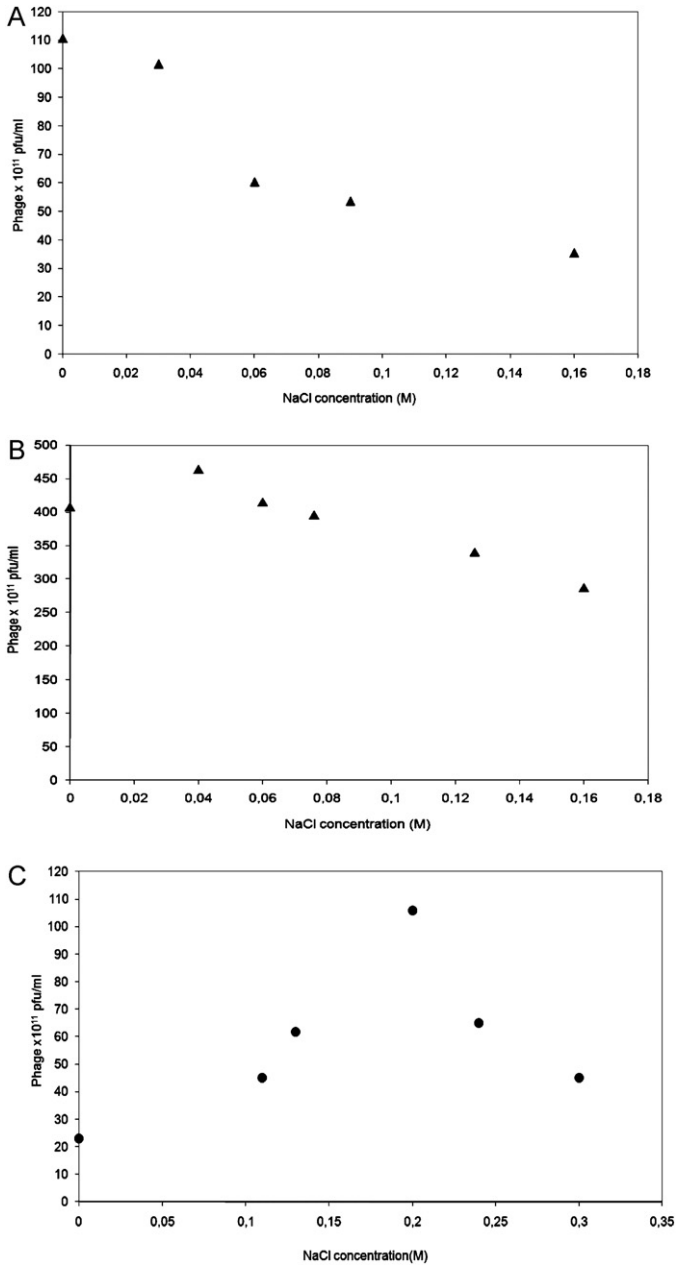

Fig. 2. Phage DBC as function of the salt concentration in the feed solution. (a) T7 phage, (b) M13 phage and (c) lambda phage. Conditions: Stationary phase: 0.034 mL CIM QA disk monolithic column; mobile phase: loading buffer: 20 mM Tris, different NaCl concentrations, pH 7.5; elution buffer: 20 mM Tris, 1.0 M NaCl, pH 7.5; flow rate: 1 mL/min; detection: UV at 280 nm. Capacities were determined at 10% of breakthrough.

When the monolithic columns are used for purification of phages it is important to determine phage recovery. Smrekar et al. [13] and Kramberger et al. [14] reported recovery between 60 and 70%, but they did not investigate effect of NaCl. Therefore, we tested if higher recovery values can be achieved. Data is shown in Fig. 3. In contrast to phages T4 and VDX-10 [13,14], we can see that recovery of M13 and T7 phage was around 100% regardless the NaCl concentration in the loading buffer, therefore efficient purification can be performed in a very broad range. This confirms that there was no irreversible binding to the matrix as well that both phages are very stable even under harsh conditions as already reported

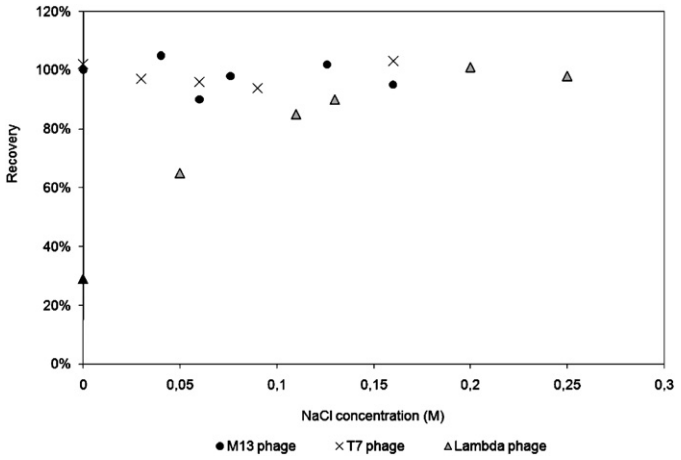

Fig. 3. Phage recovery as function of the salt concentration in the feed solution. Conditions: Stationary phase: 0.034 mL CIM QA disk monolithic column; mobile phase: loading buffer: 20 mM Tris, *x* M NaCl, pH 7.5; elution buffer: 20 mM Tris, 1.0 M NaCl, pH 7.5; flow rate: 1 mL/min; detection: UV at 280 nm. Capacities were determined at 10% of breakthrough. Recoveries were determined as titer of eluted phage divided by titer of loaded phage.

elsewhere [36]. On the other hand, recovery values are different for lambda phage, which binds the most strongly (see Fig. 1). For this phage recovery of only 30% was achieved when loaded in the absence of NaCl while this value was increasing with increase of added NaCl to reach 100% at around 0.2 M NaCl. Interestingly, this corresponds to the NaCl concentration where maximal DBC was achieved (see Fig. 2). These conditions therefore seem to be optimal for the lambda phage purification.

Alternatively to the changes of the mobile phase, recovery and capacity can also be influenced by the ligand density [22,37,38]. While lambda phage exhibited low recovery at low salt concentration and pronounced capacity optimum at 0.2 M NaCl concentration we were interested if similar trend can be achieved also with the change of the ligand density. For this purpose we prepared monoliths with 4 different densities of QA groups, namely 0.48, 0.96, 1.73 and 2.4 mmol/g, last being in the range of commercially available products [39]. To investigate only the effect of the ligand density no NaCl was added during phage loading. Capacity and recovery data are presented in Fig. 4.

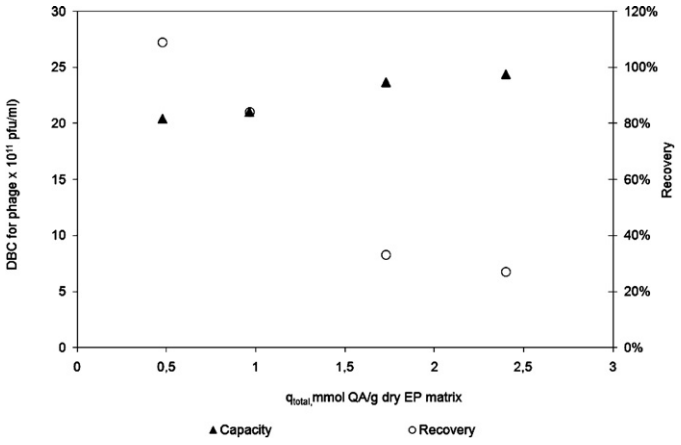

Fig. 4. Phage DBC and recovery as function of column ligand density. Conditions: Stationary phase: 0.034 mL CIM QA disk monolithic column with different ligand densities; mobile phase: loading buffer: 20 mM Tris, pH 7.5; elution buffer: 20 mM Tris, 1.0 M NaCl, pH 7.5; flow rate: 1 mL/min; detection: UV at 280 nm. Capacities were determined at 10% of breakthrough. Recoveries were determined as titer of eluted phage divided by titer of loaded phage.

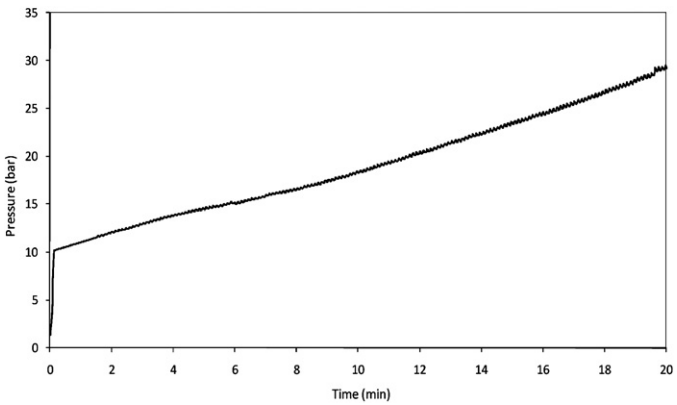

Fig. 5. Change of pressure drop on the monolithic column during loading of lambda phage. Conditions: Stationary phase: 0.034 mL CIM QA disk monolithic column; mobile phase: loading buffer: 20 mM Tris, 0.2 M NaCl, pH 7.5; flow rate: 1 mL/min; detection: UV at 280 nm.

It is interesting to notice that DBC is only slightly decreasing with a decrease of a ligand density and no optimum like in the case of changing mobile phase ionic strength occurred. This indicates that DBC optimum present at 0.2 M NaCl must be mainly due to interactions between the lambda phage particles themselves rather than due to the interactions of the phage particles with the matrix, as already predicted theoretically [21]. On the other hand, recovery substantially increased with a decrease of the ligand density, reaching 100% at the ligand density of 0.5 mmol/g of monolith. As discussed already before, addition of NaCl during loading provides 100% recovery at any ligand density.

High recoveries combined with high DBC are the main prerequisite factors to achieve high productivity of purification process. Besides, implemented flow-rate is another key parameter. While for porous particulate supports pore diffusion determines column performance and consequently the highest applicable flow-rate, for convective based media, where resolution and capacity are flow-unaffected [40], extremely high flow-rate can be implemented. Because of that, the pressure drop on the resin might become a limiting factor. During loading of the sample, molecules are loaded on the surface of the open pores decreasing their permeability [41]. As a consequence, pressure drop in the column increases. Preparative purifications are usually performed on the low pressure systems; therefore high pressure drop on the chromatographic column can result in lowering of the flow-rate and consequently decreasing the overall purification process productivity. Because of that we investigated how the loading of various phages affects pressure drop on the monolithic column. Typical data is shown in Fig. 5.

As expected, we see a substantial linear increase of the pressure from 10 to 30 bar, as a consequence of a graduate saturation of the column with the phage. Such pressure increase seems to limit use of high flow rates on the preparative scale. To estimate the effect of the pressure increase on 800 mL CIM monolithic column we evaluated decrease of the pore size using Eq. (1) and estimated to be approximately 120 nm. On 800 mL monolithic column, having higher permeability and pressure drop of 3 bar at 2000 mL/min (maximal allowed flow rate), assuming pore decrease of 120 nm the pressure would rise up to 5.5 bar what is still below the allowed maximum of 7 bar. Therefore, large monoliths can operate at its maximal productivity even under loaded conditions using e.g. protocol described elsewhere [42].

Pressure drop measurement can also provide information about adsorption behavior of molecules. Assuming that adsorbed molecules decrease pore diameter as well as the

monolith porosity [23] it is possible to estimate thickness of a formed layer from Eq. (1). While this approach was originally developed for estimation of grafted layer thickness [17], it was recently implemented for layer thickness estimation of adsorbed plasmid [26]. Using pressure drop on the loaded monolithic column at maximal DBC we can estimate phage thickness to be around 60 nm for lambda phage, around 50 nm for T7 phage and around 80 nm for M13 phage. Values for lambda and T7 phage are comparable to the phage capside size. This indicates that phage is adsorbed on the surface in a single layer and that a tail is probably spread along the surface or, because of its thinness, it does not contribute to the pressure drop increase. Detailed derivation of this conclusion is presented in Appendix A. Interestingly the thickness of adsorbed M13 phage is only of around 80 nm despite the fact that the length of the phage is 930 nm. Therefore, this hair-like phage seems to be oriented predominantly along the pore. To estimate if this is a possible option, we calculated percentage of the surface covered by the phage. Recently it was demonstrated, that a plasmid DNA loaded on the monolith to the maximal capacity has to be oriented perpendicular to the monolith surface because this is the only orientation allowing so close packing of pDNA molecules [43]. In the case of studied phages however, the surface coverage was only of few percent being the highest for the phage M13 but still only 7.5% (see Section 2.2.4). Because of that we can assume that there was no packing problem during adsorption and the orientation along the pore is feasible. Such orientation also explains why no blockage of the pores was observed during the loading.

Interesting information is obtained when we estimate adsorbed phage thickness as a function of loading conditions and dynamic binding capacity (Fig. 6). It can be seen from Fig. 6A that the estimated layer thickness was not constant but it was dependent on the loading condition. Since loading conditions also substantially affect DBC, correlation between adsorbed layer thickness and DBC is plotted in Fig. 6B. The estimated layer thickness is proportional to the amount of adsorbed phage and as already discussed approaches the phages T7 and lambda capside size at the highest capacity. Since phage capsides are rigid and therefore change of their dimensions is not expected, this is an indication that adsorbed layer at lower densities become partially permeable for the mobile phase what causes lower pressure drop increase and consequently lower value for adsorbed layer thickness. This conclusion seems to be also supported by the rather low surface coverage. One can speculate that when adsorbed layer becomes impermeable no further adsorption is possible and maximal capacity is achieved. These results are different from data for adsorption of large plasmids where the adsorbed layer was found to be impermeable for the mobile phase in a broad range of adsorbed plasmid density [26]. On the other hand, we can estimate from a linear increase of the pressure drop during the loading (Fig. 5) that in the case of tested phages amount of loaded phage determines the pressure drop on the column.

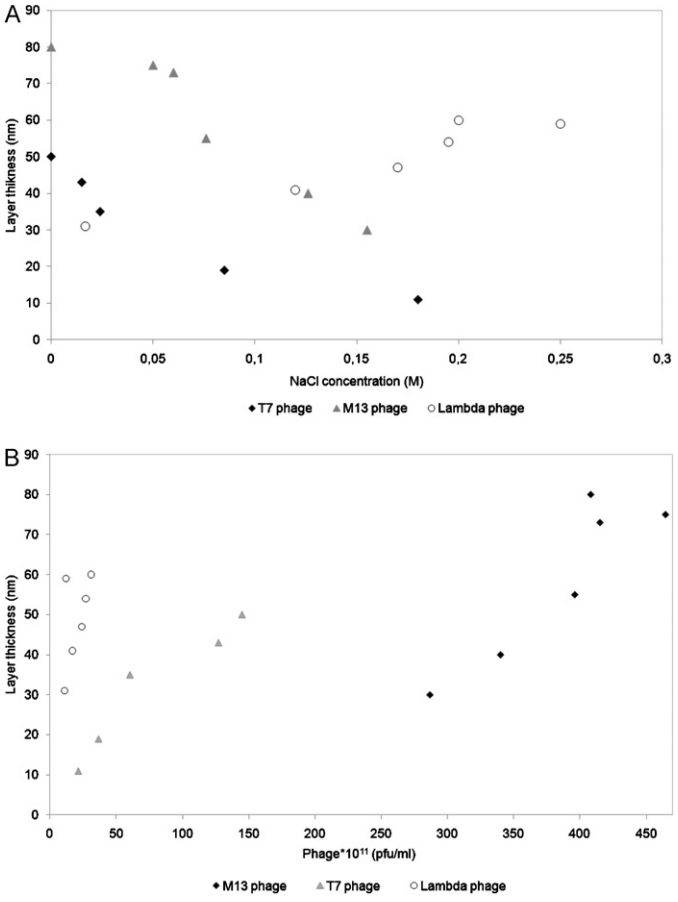

Fig. 6. (a) Layer thickness as a function of NaCl concentration. (b) Layer thickness as function of DBC. Conditions: Stationary phase: 0.034 mL CIM QA disk monolithic column; mobile phase: loading buffer: 20 mM Tris, *x* M NaCl, pH 7.5; elution buffer: 20 mM Tris, 1.0 M NaCl, pH 7.5; flow rate: 1 mL/min; detection: UV at 280 nm. Capacities were determined at 10% of breakthrough. Recoveries were determined as titer of eluted phage divided by titer of loaded phage.

4. Conclusions

Three phages exhibited very different trends of DBC when loaded at various NaCl concentrations despite being all larger than 50 nm. This indicates that for purification of specific phage screening for optimal conditions has to be performed. Measurement of a pressure drop provides insight of phage adsorption and also enables design of pressure limited large volume purification process. Because of high DBC combined with high recovery and scale independent monolithic structure, methacrylate monoliths are matrix of choice for fast determination of optimal purification conditions, which can be directly implemented on large volume monoliths to achieve highly efficient phage production.

Acknowledgements

Support of the Ministry of Higher Education, Science and Technology through programe P4-0369 is gratefully acknowledged. The Centre of Excellence for Biosensors, Instrumentation and Process Control is an operation financed by the European Union, European Regional Development Fund and Republic of Slovenia, Ministry of Higher Education, Science and Technology.

Appendix A.

To analyze orientation of the phage on the surface we estimated possible orientations of lambda phage since it is geometrically the most complex of selected ones, containing capside and rather long tail. We can discriminate between three distinct orientations as schematically presented in Fig. A1.

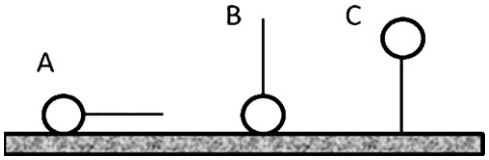

Fig. A1. Possible orientations of lambda phage adsorbed on the surface.

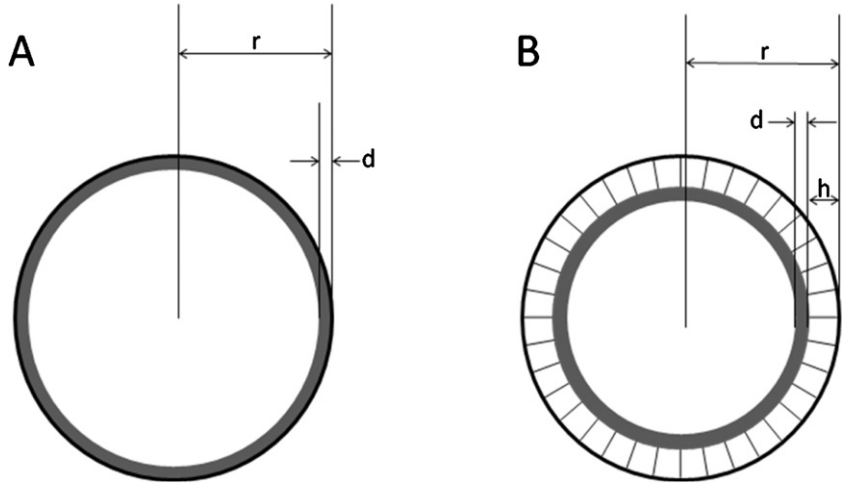

Fig. A2. Cross-section of the pore with lambda phage adsorbed in two different configurations: A – with adsorbed capside; B – with adsorbed tail

Base of the analysis is assumption that capside layer is impermeable to the flow. This is confirmed with the measurement of T7 phage being almost spherical, for which estimated value of the layer thickness and capside size match closely. Since the surface coverage density is even higher for lambda phage than for T7 phage (see main text), it is reasonable to assume that the capside layer is also impermeable for the phage lambda. Two scenarios representing two extremes are possible:

- phage tails are impermeable for the flow;
- tails do not provide any resistance to the mobile phase.

Experimental conditions under which the pressure drop was measured were identical in terms of linear velocity, viscosity and matrix, therefore

$$\frac{\Delta P_A}{\Delta P} = \frac{B}{B_A} \tag{A1}$$

Estimation of the layer thickness can in such case be derived directly from a pressure drop data according to the equation (derived from Eq. (1) by substitution with (A1)):

$$r_A = r \cdot \sqrt{\frac{\sqrt{\varepsilon^2 \cdot (\Delta P/\Delta P_A) + 4 \cdot \sqrt{\Delta P/\Delta P_A} \cdot (1-\varepsilon)} - \varepsilon \cdot \sqrt{\frac{\Delta P}{\Delta P_A}}}{2 \cdot (1-\varepsilon)}} \tag{A2}$$

We can also estimate pressure drop increase assuming certain adsorbed layer thickness according to equation derived from Eq. (A2):

$$\frac{\Delta P}{\Delta P_A} = \left(\frac{r_A}{r}\right)^8 \frac{(1-\varepsilon)^2}{\left(1-(r_A/r)^2 \cdot \varepsilon\right)^2} \tag{A3}$$

If we assume that layer of tails is impermeable, than the layer thickness would be 60nm + 120nm = 180 nm (orientation B and C), one can calculate from Eq. (A3) that the pressure drop would rise during loading from 10 bar up to approximately 300 bar instead of observed increase of up to 30 bar. Therefore, it is obvious that only orientation A gives experimentally measured pressure drop.

Second option is that the tails do provide no measureable resistance. In this case orientations A and B should exhibit the same pressure drop. One could speculate that also orientation C gives the same value but this is not the case. To elucidate the reason Fig. A2 can be helpful.

Black thin circle represents the pore surface while the grey thick circle represents capside layer. Configuration A represents actually A and B orientations from Fig. A1 while configuration B represents C orientation from Fig. A1. Since the thickness of capside layer (due to a constant capside size) is constant in both cases, B configuration occupies smaller pore volume and therefore provides lower pressure resistance. One can argue that the capside layer is denser and therefore this should result in wider capside layer thickness. However, since the surface coverage density is only around 3.3%, capsides can be easily packed in the circle with smaller diameter having slightly higher density without affecting layer thickness. The cross-section available to the flow for configuration A, Fig. A2 is therefore $S_A = \pi(r-d)^2$ where r is pore radius and d is capside layer thickness. On the other hand, cross-section of configuration B is $S_B = \pi\{r^2 - [r-h]^2 + [r-(h+d)]^2\}$, where h is phage tail length, and it is larger than S_A ($S_B - S_A = 2dh > 0$). Decrease of porosity is equal to the volume of the capside layer. Since overall pore length is equal in both cases, decrease in porosity is also proportional to the decrease of the pore cross-section due to capside layer (thick grey circle in both pictures). For lambda phage a capside size is 60 nm and tail length is 120 nm while used monolith had pore radius of 700 nm and initial porosity of 0.6. For this data calculated porosity of configuration A is 0.505 and 0.522 for configuration B. Taking available cross-section for the flow of configuration B (cross-section of an empty pore diminished for the capside layer area – grey circle) one can calculate radius of an open pore having the same cross-section area (called equivalent radius). For used monolith and phage dimensions it was calculated to be 680 nm. From Eq. (A4) (ratio of two Kozeny–Carman equations)

$$\frac{\Delta P}{\Delta P_A} = \frac{(1/d^2) \cdot ((1-\varepsilon)^2/\varepsilon^3)}{(1/d_A^2) \cdot ((1-\varepsilon_A)^2/\varepsilon_A^3)} \tag{A4}$$

inserting values of porosity and equivalent pore radius for configuration B, one gets pressure drop ratio of 0.3995 what is equivalent to the pressure drop of 25.0 bar for a loaded column, when initial pressure drop of an empty column was 10 bar. Equivalent procedure for configuration A gives expected pressure drop of 30.4 bar. If we now estimate layer thickness according to Eq. (A2) and a pressure drop of 25.0 bar we obtain value of only 49 nm. Based on this reasoning it can be concluded that only A or B orientation (Fig. A1) is possible. We should now keep in mind that capside consists of a uniform protein assembly therefore thermodynamically orientation A and B (Fig. A1) should be equivalent (assuming no interaction between tails and the matrix). This is especially true since the phage den-

sity is low (only 3% surface coverage) therefore no repulsion forces between tails are expected (e.g. brush regime in grafted layer is formed when a distance between the chains should be smaller than the chain length). Since in the case of convective flow there is some force acting on the phage tail, it is reasonable to assume that the orientation B spontaneously transforms into the orientation A. In both scenarios measured pressure drop of a loaded column indicates that orientation A is preferential.

References

[1] A. Sulakvelidze, Z. Alavidze, J.G.J. Morris, Antimicrob. Agents 45 (2001) 649.
[2] J.R. Clark, J.B. March, Trends Biotechnol. 24 (2006) 212.
[3] G.P. Smith, Science 228 (1985) 1315.
[4] J. Pande, M. Szewczyk, A. Grover, Biotechnol. Adv. 28 (2010) 849.
[5] H. Brussow, Microbiology 151 (2005) 2133.
[6] E. Kutter, A. Sulakvelidze, Bacteriophages: Biology and Applications, CRC Press, 2005.
[7] E. Creaser, A. Taussig, Virology 4 (1957) 200.
[8] L. Sundberg, S. Hoglund, FEBS Lett. 37 (1973) 70.
[9] S. Goyal, K. Zerda, C. Gerba, J. Virol. Methods 1 (1980) 79.
[10] F.E. Farber, S.E. Gradwohl, P.B. Sanford, M.J. Tobin, K.J. Lee, C.P. Gerba, J. Virol. Methods 7 (1983) 297.
[11] B. Sain, S. Erdei, Anal. Biochem. 110 (1981) 128.
[12] M. Barut, A. Podgornik, L. Urbas, B. Gabor, P. Brne, J. Vidič, S. Plevčak, A. Štrancar, J. Sep. Sci. 41 (2008) 1867.
[13] F. Smrekar, M. Ciringer, M. Peterka, A. Podgornik, A. Štrancar, J. Chromatogr. B 861 (2008) 177.
[14] P. Kramberger, R.C. Honour, R.E. Herman, F. Smrekar, M. Peterka, J. Virol. Methods 166 (2010) 60.
[15] W. Noppe, F.M. Plieva, I.Y. Galaev, K. Vanhoorelbeke, B. Mattiasson, H. Deckmyn, J. Chromatogr. A 1101 (2006) 79.
[16] W. Noppe, F.M. Plieva, K. Vanhoorelbeke, H. Deckymn, M. Tuncel, A. Tuncel, I.Y. Galaev, B. Mattiasson, J. Biotechnol. 131 (2007) 293.
[17] O. Kaltenbrunner, A. Jungbauer, J. Chromatogr. A 734 (1996) 183.
[18] I. Mihelič, T. Koloini, A. Podgornik, A. Štrancar, J. High Resolut. Chromatogr. 23 (2000) 39.
[19] M.-H. Lu, D.-Q. Lin, Y.-C. Wu, J.-X. Yun, L.-H. Mei, S.-J. Yao, Biotechnol. Bioprocess Eng. 10 (2005) 128.
[20] R.D. O'Kennedy, C. Baldwin, E. Keshavarz-Moore, J. Biotechnol. 76 (2000) 175.
[21] Y. Yuan, M.R. Oberholzer, A.M. Lenhoff, Colloids Surf. A 165 (2000) 125.
[22] M. Benčina, A. Podgornik, A. Štrancar, J. Sep. Sci. 27 (2004) 801.
[23] V. Frankovič, A. Podgornik, N. Lendero Krajnc, F. Smrekar, P. Krajnc, A. Štrancar, J. Chromatogr. A 1207 (2008) 84.
[24] E. Trilisky, A.M. Lenhoff, J. Chromatogr. A 1142 (2007) 2.
[25] N. Lendero Krajnc, F. Smrekar, J. Černe, P. Raspor, M. Modic, D. Krgovič, A. Štrancar, A. Podgornik, J. Sep. Sci. 32 (2009) 2682.
[26] N. Lendero Krajnc, F. Smrekar, A. Štrancar, A. Podgornik, J. Chromatogr. A 1218 (2011) 2413.
[27] M. Lunder, T. Bratkovič, U. Urleb, S. Kreft, B. Štrukelj, Biotechniques 44 (2008) 893.
[28] S. Cabilly, Mol. Biotechnol. 12 (1999) 143.
[29] T. Dokland, H. Murialdo, J. Mol. Biol. 233 (1993) 682.
[30] G.C. Lander, A. Evilevitch, M. Jeembaeva, C.S. Potter, B. Carragher, J.E. Johnson, Structure 16 (2008) 1399.
[31] V.I. Permogorov, B.V. Taglov, V.G. Bogush, V.E. Minaev, Sov. Mol. Biol. 11 (1977) 134.
[32] I. Mihelič, D. Nemec, A. Podgornik, T. Koloini, J. Chromatogr. A 1065 (2005) 59.
[33] G. Ronto, M.M. Agamalyan, G.M. Drabkin, L.A. Feigin, Y.M. Lvov, Biophys. J. 43 (1983) 309.
[34] S.A. Berkowitz, L.A. Day, J. Mol. Biol. 102 (1976) 531.
[35] R.D. Dyson, K.E. Van Holde, Virology 33 (1967) 559.
[36] M. Balass, E. Morag, E.A. Bayer, S. Fuchs, M. Wilchek, E. Katchalski-Katzir, Anal. Biochem. 243 (1996) 264.
[37] J. Urthaler, R. Schlegl, A. Podgornik, A. Strancar, A. Jungbauer, R. Necina, J. Chromatogr. A 1065 (2005) 93.
[38] M. Barut, A. Podgornik, M. Merhar, A. Štrancar, in: F. Švec, T.B. Tennikova, Z. Deyl Z (Eds.), Monolithic Materials: Preparation, Properties and Applications, Elsevier, Amsterdam, 2003, p. 51.
[39] http://www.biaseparations.com/pr/260/362/specific-information.
[40] A. Podgornik, M. Barut, S. Jakša, J. Jančar, A. Štrancar, J. Liq. Chromatogr. Relat. Technol. 25 (2002) 3097.
[41] A.I. Liapis, J.J. Meyers, O.K. Crosser, J. Chromatogr. A 865 (1999) 13.
[42] F. Smrekar, M. Ciringer, M. Peterka, P. Raspor, A. Štrancar, A. Podgornik, MSS 2008, Portorož, 2008.
[43] C. Tarmann, A. Jungbauer, J. Sep. Sci. 31 (2008) 2605.